



## OPEN ACCESS

## EDITED BY

Konstantinos Topouzelis,  
University of the Aegean, Greece

## REVIEWED BY

Ana Laura Delgado,  
CONICET Instituto Argentino de  
Oceanografía (IADO), Argentina  
Milad Niroumand-Jadidi,  
Bruno Kessler Foundation (FBK), Italy

## \*CORRESPONDENCE

Helder Arlindo Machaieie  
machaielder@gmail.com

## SPECIALTY SECTION

This article was submitted to  
Coastal Ocean Processes,  
a section of the journal  
Frontiers in Marine Science

RECEIVED 16 March 2022

ACCEPTED 13 July 2022

PUBLISHED 12 August 2022

## CITATION

Machaieie HA, Nehama FPJ, Silva CG  
and de Oliveira EN (2022) Satellite  
assessment of coastal plume variability  
and its relation to environmental  
variables in the Sofala Bank.  
*Front. Mar. Sci.* 9:897429.  
doi: 10.3389/fmars.2022.897429

## COPYRIGHT

© 2022 Machaieie, Nehama, Silva and  
de Oliveira. This is an open-access  
article distributed under the terms of  
the [Creative Commons Attribution  
License \(CC BY\)](https://creativecommons.org/licenses/by/4.0/). The use, distribution  
or reproduction in other forums is  
permitted, provided the original  
author(s) and the copyright owner(s)  
are credited and that the original  
publication in this journal is cited, in  
accordance with accepted academic  
practice. No use, distribution or  
reproduction is permitted which does  
not comply with these terms.

# Satellite assessment of coastal plume variability and its relation to environmental variables in the Sofala Bank

Helder Arlindo Machaieie<sup>1\*</sup>, Fialho Paloge Juma Nehama<sup>1</sup>,  
Cleverson Guizan Silva<sup>2</sup> and Eduardo Negri de Oliveira<sup>3</sup>

<sup>1</sup>Department of Marine Science, School of Marine and Coastal Sciences, Eduardo Mondlane University, Quelimane, Mozambique, <sup>2</sup>Department of Geology and Geophysics, Institute of Geosciences, Fluminense Federal University, Niterói, Brazil, <sup>3</sup>Department of Physical Oceanography, Faculty of Oceanography, Rio de Janeiro State University, Rio de Janeiro, Brazil

Monthly composites of remote sensing reflectance at 555 nm wavelength ( $R_{rs555}$ ) from ocean color imagery of the MODIS sensor onboard the Aqua platform were used to characterize the spatial and temporal variability of coastal plume in the Sofala Bank and its relation to river discharge, local rainfall, and wind speed. To achieve the objective, maps of monthly composites of  $R_{rs555}$  over the Sofala Bank were inspected and statistical analysis was performed, including correlation, analysis of variance, and wavelet coherence between environmental variables and both plume area and  $R_{rs555}$ . Climatology of  $R_{rs555}$  revealed that both plume dispersion and  $R_{rs555}$  values are higher during June to December and lower during January to May. A positive correlation ( $r = 0.77$ ) between wind speed and monthly time series of  $R_{rs555}$ , and a negative correlation between the Zambezi river discharge ( $r = -0.21$ ) and rainfall ( $r = -0.67$ ) with  $R_{rs555}$  were found. These results suggest that variation of suspended matter in the Sofala Bank is mainly controlled by erosion and re-suspension by winds rather than the input of terrigenous matter by the Zambezi River discharge and rainfall, assuming that  $R_{rs555}$  can be a valid proxy for the inorganic suspended matter. The southern portion of the Sofala Bank (i.e., near the mouths of the Pungue and Buzi Rivers) presented higher values of  $R_{rs555}$  if compared to the center region near Zambezi river mouth and the northern region near Licungo river mouth. The higher  $R_{rs555}$  values in the southern region might be associated with higher re-suspension rates due to increased tide mixing, dredging activities, and the shallower nature of bathymetry in the southern region. The dominance of wind in controlling the variability of suspended sediments and the eventual relatively greater contribution of Pungue and Buzi River than the Zambezi in supplying sediments could represent an evidence of weakening of Zambezi River supply of sediments, a process that might have started after damming the Zambezi Catchment.

## KEYWORDS

Sofala Bank, coastal plume, remote sensing,  $R_{rs555}$ , Mozambique shelf

## Introduction

Coastal plumes are in many cases characterized by high concentrations of suspended matter brought to the marine environment by river discharges. River discharges influence physical and biogeochemical processes, as well as the primary production of continental shelves worldwide because freshwater and the range of matter (i.e., organic, inorganic, dissolved, and particulate) brought to the marine environment directly impact the stratification and light attenuation in the water column, and provide the necessary nutrients to support primary production (Lihan, et al., 2008; Piola et al., 2008). The plume dynamics is driven by a variety of factors such as river discharge, wind stress, waves, buoyancy currents, and tidal currents (Durand et al., 2002; Warrick, et al., 2007; Liu, et al., 2008). After a long period of special attention to plumes from large rivers such as Amazon, Mississippi and La Plata, there has been a significant increase in recent decades of studies addressing smaller plumes (e.g., Siddorn et al., 2001; Nezlin et al., 2005; Warrick, 2007), in recognition of their relevance argued by the higher ratio of plume area to discharge rate (Warrick and Fong, 2004).

The freshwater and its respective suspended matter supplied by Zambezi, Licungo, Buzi, and Pungue rivers in the Sofala Bank, located along the western side of Mozambique Channel, are believed to have high influence in secondary coastal production (Lutjeharms, 2006; Nehama, 2012), and therefore understanding its variability is of great importance. Despite its importance, as far as we know, the seasonal and interannual variability of the suspended matter in the Sofala Bank and its current main forcing have not been studied. In addition, the influence of the dams on the Zambezi discharge variability was not yet fully investigated.

Over the last few decades, studies of coastal plumes have shown that satellite remote sensors can provide better spatial and temporal coverage in comparison to what is possible to achieve with the traditional observation methods. Remote sensors can distinguish most plumes from ambient seawater because they often differ in color, turbidity, salinity, or temperature (Klemas, 2012). Some of the studies have focused on establishing empirical or semi-empirical bio-optical relationships to retrieve near-surface biogeochemical parameters like suspended sediment, dissolved organic matter, turbidity, and salinity, using the remote sensing reflectance ( $R_{rs}$ ) as a proxy (Siddorn et al., 2001; Gholizadeh et al., 2016; Balasubramanian et al., 2020; IOCCG, 2020).

Bontempi and Yoder (2004) also used optical properties in the green spectral region to study chlorophyll-a fronts. As stated by the authors, water-leaving radiance ( $L_w$ ,555) front is an optical signature of the transition from waters of high backscatter (high suspended matter) to low backscatter (low suspended matter). Other studies that used  $R_{rs,555}$  to map coastal plumes include Nezlin and DiGiacomo (2005); Jabbar et al. (2013), and Saldias et al. (2016).

Remote sensing data are affected by errors and uncertainties, same as with any other observational data. Some factors that have a significant influence on the accuracy of remote sensing data are as follows: correction of the atmospheric influence; bio-optical model, which is the basis of the retrieval algorithm; the vertical distribution of the quantity to be derived along with the vertical penetration depth of the radiation in the spectral bands, which are used in the algorithm; sub-pixel patchiness of the water constituents; uncertainties in *in situ* data used for calibration and considered as “true values”; and different water bodies represented in *in situ* and remotely sensed data (IOCCG, 2019).

Specifically, uncertainties in satellite measurement of  $R_{rs}$  are approximately of 5%–15% in the blue and green regions and can vary as a function of the water-column optical complexity (Hu et al., 2013; IOCCG, 2019; Alikas et al., 2020). The main sources of  $R_{rs}$  errors are the procedures used to correct the atmospheric contamination, and the performance of bio-optical models is expected to degrade for large uncertainties in  $R_{rs}$ . For instance, Balasubramanian et al. (2020) introduce a hybrid scheme for total suspended solid (TSS) retrievals that would advance the state of the art for TSS retrievals in both inland and coastal waters. They demonstrate that 10% uncertainties in  $R_{rs}$  ( $600 \text{ nm} < \lambda < 800 \text{ nm}$ ) result in ~20% uncertainties in TSS, and although their model performs better than existing algorithms, there still remains about 80% error in global TSS retrievals.

Due to scarcity of *in situ* data from the Sofala Bank to verify the accuracy of global models, we hereby propose to evaluate the dynamics of coastal plume using the remote sensing reflectance centered in the green spectral band, namely, 555 nm. The advantage of applying this band in low and moderate turbidity waters is threefold. Firstly, the  $R_{rs,555}$  indicates an optical signature dominated by the transition from waters of high to low backscatter. Light absorption by water is lowest in the green spectrum, allowing the radiation to interact with the suspended matter even in water with low sediment concentration. Secondly,  $R_{rs,555}$  is the portion of the water-leaving reflectance spectrum that is relatively independent of pigment concentration. Lastly,  $R_{rs,555}$  is the portion of the water-leaving reflectance spectrum that is relatively independent of pigment concentration (Bontempi and Yoder, 2004). Additionally, the potential of the green band for mapping coastal plume waters is denoted by the strong correlation between scattering at this band and both concentration of suspended sediments and salinity (Siddorn et al., 2001). Siddorn et al. (2001) also pointed out that the behavior of light in the Sofala Bank is dependent on the scattering by inorganic particulate material and the absorption by yellow substances. However, it is worth mentioning that colloidal material can also be a contributor to the scattering; a compounding factor is that a relevant part of the colloids goes through the filters typically used to distinguish the dissolved and particulate parts found in water (Stramski and Wozniak, 2005). Toole and Siegel (2001) evaluated the correlation between water

quality parameters and remote sensing reflectance in Santa Barbara Channel and observed that the spectral band that best correlates with lithogenic silica (which is one of the elements of terrigenous sediments) was the green band (555 nm). Tan et al. (2006) found a strong positive correlation ( $r = 0.84$ ) between normalized water leaving radiance at 555 nm ( $nLW_{555}$ ) and *in situ* suspended sediments in the Malacca Straits. On the other hand, Saldías et al. (2016) correlated a time series of surface salinity and  $nLW_{555}$  in a hydrographical station located within the river plumes off central-southern Chile and found a significant negative correlation ( $r = -0.75$ ,  $p < 0.05$ ).

When applying the green band to map coastal plumes, it is assumed that the plume area is proportional to the number of pixels within the plume limited by a threshold value of  $R_{rs,555}$  or  $nLW_{555}$ , while the plume intensity is proportional to the mean value of  $R_{rs,555}$  or  $nLW_{555}$  estimated from pixels within the plume area (Nezlin and DiGiacomo, 2005). On the other hand, taking into consideration that the plume results from rainfall on the watershed and river discharge, it is reasonable to consider the variation of the plume area and plume intensity as being proportional to the variations in rainfall and river discharge. Based on this approach, Nezlin and DiGiacomo (2005) determined the value of the  $nLW_{555}$  representative to plume edge (i.e., outer boundary) by correlating different  $nLW_{555}$  thresholds and accumulated rainwater over the coast of San Pedro. These authors selected the threshold value that best correlated to rainwater as the value of  $nLW_{555}$  in the plume outer edge. This approach was subsequently applied successfully in other studies, such as Saldías et al. (2012); Jabbar et al. (2013), and Mendes et al. (2017). In all these studies, the river was found to be the main driver of plume variability, with the winds playing a secondary role. However, taking into account that currently the Zambezi river runoff, which is the most important river draining in the Sofala Bank, does not show significant seasonal variation (Machaieie, 2018), and the sediments are retained in the dam, we hypothesize that winds can play a major role on the variability of suspended sediments in the Sofala Bank. Thus, in the present study, monthly remote sensing reflectance at 555 nm from MODIS ocean color imagery is used to characterize the spatial and temporal variability of suspended sediment plume produced by the Zambezi River in the Sofala Bank, using the method proposed by Nezlin and DiGiacomo (2005) and testing the role of local winds in driving the plume variability.

## Study area

The Sofala Bank (Figure 1) is a shallow and large continental shelf located in the central region of the Mozambique coast, extending from Angoche at 17°S to Nova Mambone near 21°S. It is the largest continental shelf of the East African coast with an area of nearly 50,000 km<sup>2</sup>. The

productivity of the Sofala Bank is highly enriched by the terrigenous input of nutrients from Zambezi River (Lutjeharms, 2006; Kolasinski et al., 2012), one of the largest rivers in Africa, and also by extensive mangroves that provide shelter and nursery ground for important fisheries and crustacean. According to Hogueane (2007), the climate in the region is humid subtropical with two seasons, a dry and cold season during May to September, and a hot and wet season during October to March. The Sofala Bank hosts the largest tides in the western Indian Ocean (Pugh, 1987; Chevane et al., 2016), with tidal ranges reaching about 6.4 m during spring tides, whereas outside the bank, the southern and northern Mozambique shelf have tidal ranges of about 3 m (Hogueane, 2007). The morphology of the coastal zone of the Sofala Bank is characterized by flat land with an almost continuous fringe of mangrove swamps (Hogueane, 2007), and the seabed morphology in the central and northern Sofala Bank is flat, whereas the southern part of the bank is characterized by sandwaves due to strong tidal currents and waves (WWF, 2004; Flemming and Kudrass, 2017). The Sofala Bank presents an estuarine environment due to the influence of freshwater from Zambezi River, which discharges at about 3,000 m<sup>3</sup>/s on average (Gammelsrod, 1996; Siddorn et al., 2001) contributing to almost 85% of the total freshwater discharged in the Sofala Bank. The Zambezi annual runoff has reduced markedly since 1976 (Beilfuss and dos Santos, 2001) when the difference between wet and dry season flows became less significant because of the river regulation at Cahora Bassa dam. The brackish water may move over oceanic water to about 50 km offshore and may extend to the full depth of water column, presumably because of the shallow nature of the bank, combined with the effect of winds and tides (Lutjeharms, 2006; Nehama, 2012). At the southern end of the bank, between 20° and 21°S, there is a large extent of coastline subjected to inundation by seawater as result of extreme evaporation and over-transpiration in the mangrove swamps and salt marshes (Silvada, 1984). The circulation in the Sofala Bank is influenced by the passage of south going eddies in the Mozambique Channel (Lutjeharms et al., 2012; Halo, et al., 2014), offshore the 50-m isobaths (Schulz et al., 2011). At the coast, the main feature is a north-going surface current (Saetre, 1985; Machaieie, 2012), presumably forced by the prevailing southeasterly winds. The tides also play a role in coastal circulation of the Sofala Bank, especially during spring tides, when barotropic tidal currents with up to 70 cm s<sup>-1</sup> can be found in the central region of the Bank (Chevane et al., 2016).

Fine particles are transported by the longshore current system and deposited in two areas: (1) at the nearshore to northeast covered by muds with up to 50% sand, and (2) at the outer shelf below 60 m depth covered by muddy sand with the mud content increasing towards the open waters (Schulz et al., 2011). Sediment transport at shallow depths is also affected

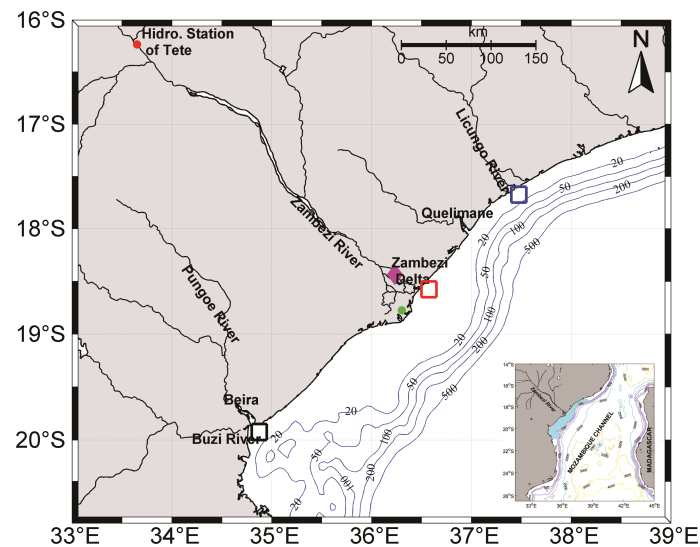


FIGURE 1

Map showing the study area. The black, red, and blue boxes are the small domains used to compare the suspended sediment concentrations in southern, central, and northern regions of the Sofala Bank. The green point represents the area of the wind speed time series. The magenta box represents the area of rainfall time series.

by wave action and tidal currents, heavily influenced by monsoonal onshore winds and freshwater input from the hinterland (Nehring et al., 1987). Previous studies using satellite data for assessing the plume dynamics in the Sofala Bank have used optical properties from a dataset collected in April of 1998 (Siddorn et al., 2001). These authors developed an empirical relationship between the salinity and a reflectance ratio centered in the spectral region of green ( $R_{rs555}/R_{rs490}$ ), with the caveat that the algorithm could fail in the event of a high primary productivity. According to these authors, it is the yellow substance (and water) that dominates light absorption, and inorganic solids that dominate light scattering in the Sofala Bank waters, at least during that specific field campaign. The mean concentration values for total suspended material, particulate inorganic material, particulate organic material, chlorophyll, and yellow substance were  $2.4 \text{ mg L}^{-1}$ ,  $0.7 \text{ mg L}^{-1}$ ,  $1.8 \text{ mg L}^{-1}$ ,  $0.13 \text{ mg m}^{-3}$ , and  $0.19 \text{ mg L}^{-1}$ , respectively. As pointed out in their paper, the low concentrations of suspended material may be a result of the dams.

According to Nehama et al. (2015), four water masses are found in the Sofala Bank, namely, Low Salinity Shelf Waters, Warmer Oceanic Surface Waters, Deep Oceanic Waters, and High Salinity Shelf Waters. The Low Salinity Shelf Waters are observed at the upper 15 m within 40 km from coastline. The Warmer Oceanic Surface Waters occur throughout the bank, at depths not exceeding 70 m. The Deep Oceanic Waters are observed from the sub-surface layer to the seabed. The High Salinity Shelf Waters are observed offshore, more than 40 km from the coastline, at depths greater than 15 m.

## Data and methods

### Satellite-derived remote sensing reflectance

A total of 168 MODIS-Aqua Level-3 monthly mean remote-sensing reflectance ( $R_{rs}$ , 555 nm) data, for the period between 2003 and 2016, processed with updates in calibration and algorithms (reprocessing R2014.0), were obtained from the NASA Ocean Biology Processing Group (OBPG, <http://oceancolor.gsfc.nasa.gov/>). The satellite data were made available in the NetCDF format and were processed in Matlab, version 8.1 (R2013a). The initial data processing consisted in creating spatial  $R_{rs555}$  time series for a region covering the study area (Figure 1).

### River discharge and rainfall data

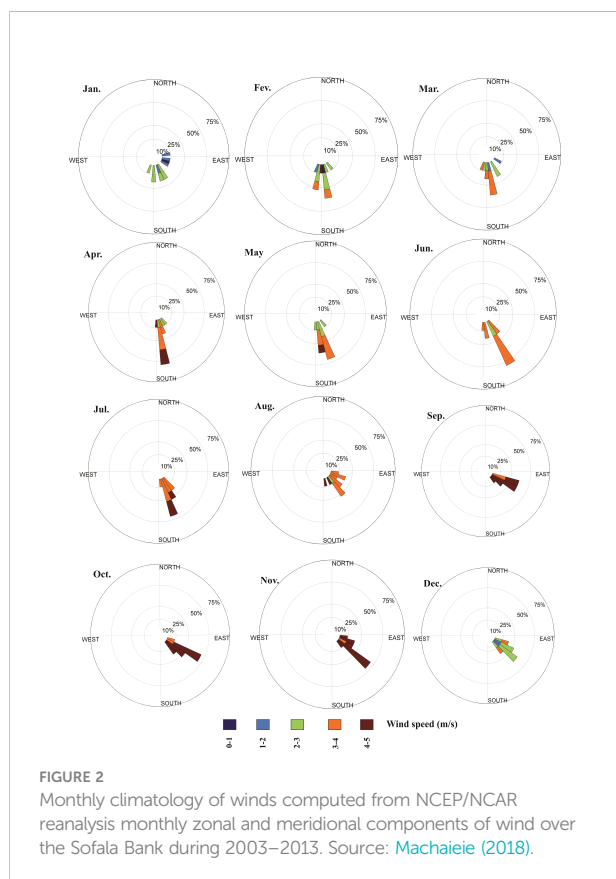
Monthly means of the Zambezi river discharge were provided by the national directorate for water affairs of Mozambique. The data were measured at the Tete hydrographic station, located at about 440 km upstream from the main Zambezi river mouth (Figure 1). Monthly rainfall data from the Tropical Rainfall Measuring Mission (TRMM), with  $0.5^\circ$  spatial resolution were obtained from the NASA web site (<https://giovanni.gsfc.nasa.gov/giovanni/>). Details of TRMM mission are given in Huffman et al. (2007). The data were selected for a subset area of the Sofala Bank in the vicinity of the main mouth of the Zambezi River (magenta box in Figure 1).

## Wind speed

Monthly zonal and meridional components of wind from NCEP/NCAR reanalysis (Kalnay et al., 1996) measured at 10 m above the surface with 2.5° spatial resolution were downloaded from the website of the National Center for Environmental Prediction (NCEP, <https://www.esrl.noaa.gov/>). After interpolation to a 0.25° grid, a time series for the point 36.25° E and 18.75° S was made assuming that wind intensity and direction immediately in front of the Zambezi mouth are representative of the entire study area. This assumption is based on the fact that the wind does not present significant spatial variability in the study area (Sætre and Jorge de Silva, 1982; Machaieie, 2018). Machaieie (2018) computed wind rose from the monthly average of NCEP/NCAR reanalysis for the Sofala Bank and found southeasterly and southerly winds occurring in the Sofala Bank, with southeasterly being the most prevailing and most intense winds (Figure 2).

## Determination of plume edge and plume area

The basic concept is that the variation in the area covered by sediment plume and its intensity are forced by river discharge,



rainfall, and wind stress through sediment input (by the river and rainfall drainage from the watershed), dispersion, erosion, and re-suspension of sediments (by wind stress). To identify the value of  $R_{rs555}$  that best characterizes the plume edge, for each image, spatial areas of different thresholds of  $R_{rs555}$  edge values were correlated to river discharge, rainfall, and wind, which are assumed to be the main forcings. The values of  $R_{rs555}$  thresholds varied from 0.0025 to 0.02  $Sr^{-1}$ . The  $R_{rs555}$  threshold that presented the maximum correlation with one or a combination of the forcings (river discharge, rainfall, and wind speed) was taken as sediment plume edge. This approach is similar to that used in previous studies about river plumes (e.g., Nezlín and DiGiacomo, 2005a; Saldías et al., 2016; Fernandez-Nóvoa et al., 2017). It is worth noting, however, that the approach is somehow subjective since there is no standard rule for threshold spacing or range, and the limits of variation of reflectance or normalized water leaving radiance vary from one area to another. The plume area was calculated by counting the number of pixels with  $R_{rs555}$  values equal or above the threshold and multiplying by pixel size.

## Variation of plume morphology

In order to access the annual variation of coastal plume morphology in the Sofala Bank, maps presenting monthly climatology of  $R_{rs555}$  and ensemble mean  $R_{rs555}$  within the whole plume area were analyzed. Additionally, an average of  $R_{rs555}$  in each of the three  $22 \times 22$  km boxes (Figure 1) located near Pungue and Buzi river mouth (in the south), Zambezi Delta (in the center), and Licungo River mouth (in the north) was determined. These  $R_{rs555}$  monthly time series were used to access the temporal variability of coastal plume in the Sofala Bank as a whole, and later compared with the plume variability in the south, center, and north regions.

The relation between the variation of coastal plume and river discharge, rainfall in the Zambezi Delta, and wind speed was accessed through three different analyses, namely, overlapping their annual and interannual variation, correlation analysis, one-way analysis of variance (ANOVA), and wavelet transform coherence (WTC) using a Matlab software package developed by Grinsted et al. (2004). The one-way ANOVA was performed to evaluate the significance of differences among the groups following the description in Weiss (2006). The WTC analysis was performed with the aim of complementing the correlation analysis, since WTC allows the identification of moments when the two time series vary concurrently.

## Results and discussion

Figure 3 shows the statistical results for the plume edge estimate through regression of  $R_{rs555}$  thresholds to river

discharge, rainfall, and wind speed. The best correlation coefficients for river discharge and rainfall are 0.25 and 0.5 and are located at the  $0.01 \text{ Sr}^{-1}$  threshold. The maximum correlation between wind speed and  $R_{rs555}$  thresholds is 0.6 and is found at three  $R_{rs555}$  thresholds, namely, 0.0075, 0.01, and  $0.0125 \text{ Sr}^{-1}$ . The correlation coefficient from multiple linear regression between the combination of the three forcings and thresholds of plume edge is maximum at  $0.01 \text{ Sr}^{-1}$ ; therefore, the  $R_{rs555} = 0.01 \text{ Sr}^{-1}$  threshold is taken as the mean plume edge in the Sofala Bank.

The seasonal variation of plume extension and the  $R_{rs555}$  intensity (assuming that it is a proxy to suspended matter concentration) is presented in Figure 4, and it shows two main regimes for both plume extension and  $R_{rs555}$  signal. From January to March, the plume area, limited by  $0.01 \text{ Sr}^{-1}$  threshold, is much confined to the coast and the  $R_{rs555}$  values are low, varying between  $0.008$  and  $0.01 \text{ Sr}^{-1}$  inside the plume area. During July–December, the plume extension is relatively wider and sediment concentration is relatively higher, as indicated by  $R_{rs555}$  values varying between  $0.01$  and  $0.014 \text{ Sr}^{-1}$  in the plume area. From June to December, there are also occurrences of small plumes characterized by considerably high values of  $R_{rs555}$  near the mouths of Licungo and Pungue rivers, in the north and south portions of the study area, respectively. It must be noted that the monthly mean composites mask the hourly, daily, and weekly variations in both plume extent and concentration of suspended matter in such a way that in those time scales, the maximum plume extension might be located further offshore. The center portion, where the main mouths of the Zambezi delta are located, presents lower values of  $R_{rs555}$  if compared to the north and south portions, suggesting the occurrence of lower concentrations of suspended matter. The

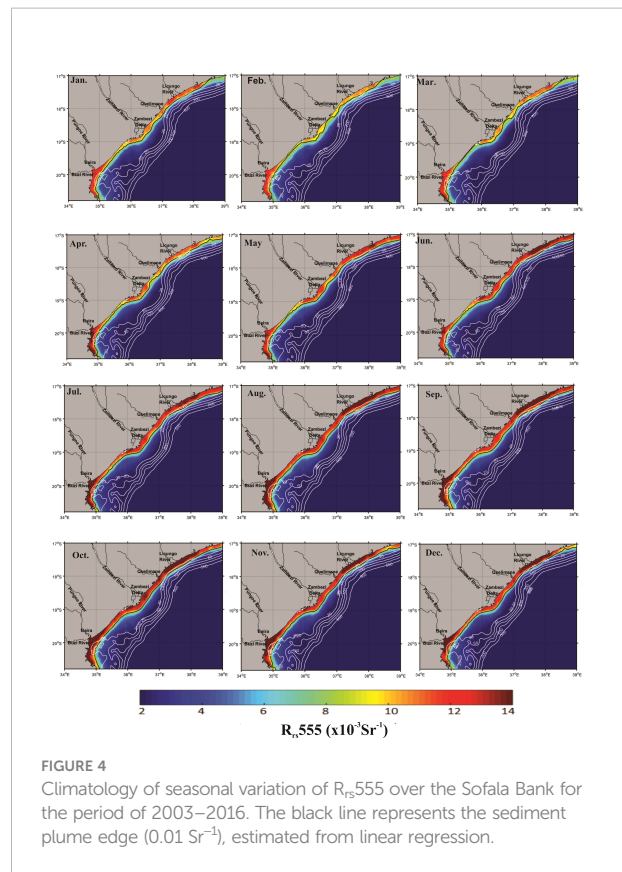


FIGURE 4  
Climatology of seasonal variation of  $R_{rs555}$  over the Sofala Bank for the period of 2003–2016. The black line represents the sediment plume edge ( $0.01 \text{ Sr}^{-1}$ ), estimated from linear regression.

location of the smaller plumes in relation to their respective river mouths suggest that the formation of those plumes is not linked to the Zambezi river discharge, despite this being the most important river draining in the Sofala Bank. On the other

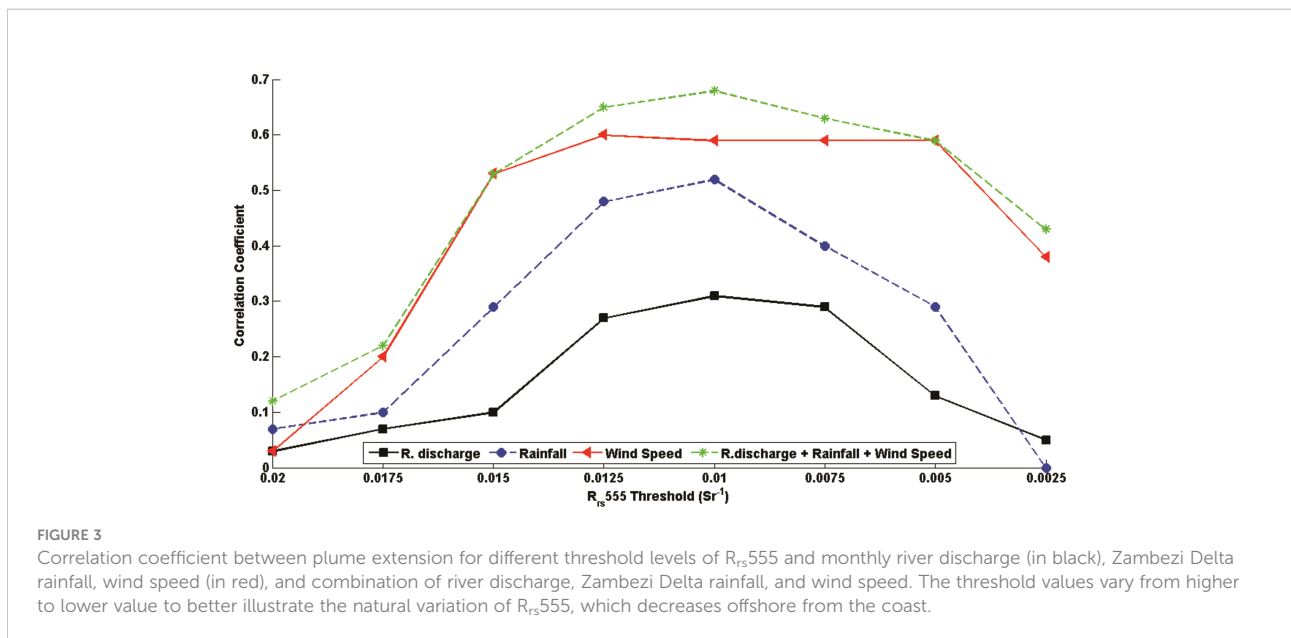


FIGURE 3  
Correlation coefficient between plume extension for different threshold levels of  $R_{rs555}$  and monthly river discharge (in black), Zambezi Delta rainfall, wind speed (in red), and combination of river discharge, Zambezi Delta rainfall, and wind speed. The threshold values vary from higher to lower value to better illustrate the natural variation of  $R_{rs555}$ , which decreases offshore from the coast.

hand, the period between June and December characterized by wider plume and high values of  $R_{rs555}$  is also characterized by relatively lower river discharge from the Zambezi and high wind speed, as observed by Machaieie (2018).

Figure 5 presents the climatology of the annual variation of plume area and  $R_{rs555}$  signal intensity in the plume area overlapped with annual variations of the Zambezi River discharge, rainfall in the Zambezi Delta, and wind speed. It is possible to note that both plume area and  $R_{rs555}$  values are more directly related to wind speed rather than river discharge and rainfall. Although it does not present large variations between the minimum and maximum flows, the Zambezi river discharge still has two distinct regimes. The high flow regime extends between December and April with mean discharge values varying between  $2,100 \text{ m}^3 \text{ s}^{-1}$  in April and about  $2,600 \text{ m}^3 \text{ s}^{-1}$  in February and the low flow regime extends between May and November with a minimum value of about  $1,800 \text{ m}^3 \text{ s}^{-1}$  in August. The rainfall exhibits a pattern that is similar to the Zambezi River discharge, but with 1 month of lagging time for the maximum value. The time difference might be a result of damming the Zambezi river flow, or the fact that the flow measured 440 km upstream results from the precipitation in the entire Zambezi River basin that is non-uniform over the nearly  $1.39 \times 10^6 \text{ km}^2$ .

The variation of plume area and  $R_{rs555}$  also shows two main regimes, whose temporal sequence is almost an inversion of that of the Zambezi River discharge and rainfall in the Zambezi Delta. The peak regime of plume area and  $R_{rs555}$ , with values varying between  $1.2$  and  $2 \times 10^4 \text{ km}^2$ ,  $0.0125$  and  $0.137 \text{ Sr}^{-1}$ , respectively, extends from June to December with the maximum in October. The low regime occurs from January to

May. The wind speed, in its turn, shows a similar variation to  $R_{rs555}$ , with a gradual increase from  $2.6 \text{ m s}^{-1}$  in January to its peak in October, followed by a steep decrease to about  $2.8 \text{ m s}^{-1}$  in December. The quasi-inverse relation between the annual variation of the Zambezi River discharge and both plume area and  $R_{rs555}$  signal is an indication that although the river discharge might still be the main source of suspended sediments from outside the bank, the temporal modulator is the wind, probably *via* re-suspension. The current disconnection between the Zambezi river discharge and the variation of the  $R_{rs555}$  signal might be due to the actual low seasonal signal of the Zambezi river discharge resulting from regulation of the flow in the Cahora Bassa dam. Machaieie (2018) compared the annual variation of the Zambezi river discharge at Tete station for the periods before and after the construction of Cahora Bassa dam and found that the actual difference between maximum monthly mean flow corresponds to only 20% of  $4000 \text{ m}^3 \text{ s}^{-1}$  observed before the regulation of the flow in Cahora Bassa dam. Davies et al. (2000) observed a dramatic change in the morphology of the river floodplain system during surveys conducted in Zambezi Delta in 1996, which might reflect on the current non-linkage between the river discharge and concentration of suspended sediments. Ronco et al. (2010) predicted coastal erosion in the Zambezi Delta as a consequence of damming. The coastal erosion along with re-suspension forced by wind and wind-generated waves might be the main source of suspended sediments.

The findings of Figures 4, 5 corroborate with the overlap of time series of forcing parameters and mean  $R_{rs555}$  within the plume area presented in Figure 6. It is possible to note that the monthly time series suggests that the variation in  $R_{rs555}$  is

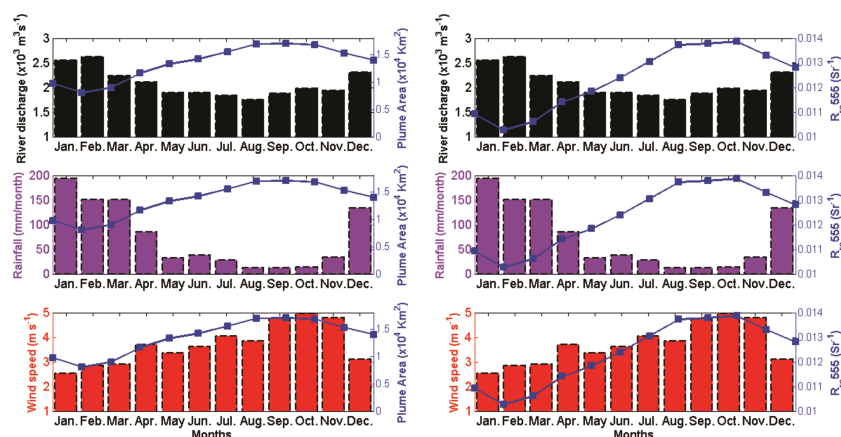


FIGURE 5

Overlap of the climatology of annual variation of the Zambezi River discharge with plume area and  $R_{rs555}$  (upper), rainfall with plume area and  $R_{rs555}$  (middle), and wind speed with plume area and  $R_{rs555}$  (lower) for the 2003–2016 period. The monthly mean  $R_{rs555}$  used to compute the seasonal climatology was extracted from the mean plume area estimated through linear regression. .

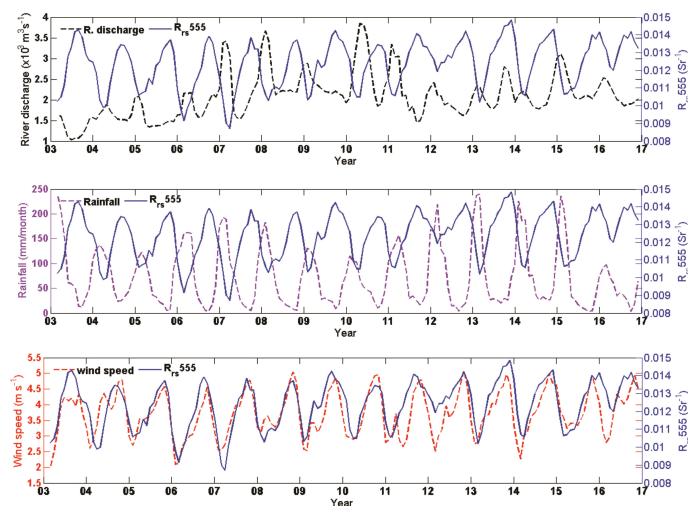


FIGURE 6

Overlap of monthly time series of river discharge with  $R_{rs555}$  (upper panel), rainfall in Zambezi Delta with  $R_{rs555}$  (middle panel), and wind speed with  $R_{rs555}$  (lower panel).

directly linked to wind speed, in analogy to the annual variation shown in Figures 4 and 5. While the river discharge and rainfall present high values in Austral summer and low values in winter without showing any correlation to  $R_{rs555}$ , the wind speed shows a clear correlation to  $R_{rs555}$  and they both show an inverted pattern when compared to that of river discharge and rainfall, presenting high values during winter and lower values in Austral summer. In addition, the WTC results for rainfall– $R_{rs555}$  and wind speed– $R_{rs555}$  show a  $180^\circ$  and  $0^\circ$  phase difference, respectively (Figure 7, upper and lower panels), for the 8- to 16- and 3- to 16-month time scale, indicating an asynchronous relationship between rainfall and  $R_{rs555}$  and a synchronous relationship between wind speed and  $R_{rs555}$ . In contrast, the result for river discharge– $R_{rs555}$  WTC does not show a single continuous relationship (Figure 7, middle panel) throughout the period in analysis. High asynchronicity is found between months 20 and 60 when the correlation is notably higher with a phase difference of about  $90\text{--}135^\circ$ . The difference changes to about  $90^\circ$  between months 120 and 140. Between months 60 and 120, the relationship is weak, as indicated by the values of correlation coefficient is below 0.5.

The linkage between the variability of wind speed and  $R_{rs555}$  is also demonstrated by correlation coefficients presented in Table 1, which shows a significant positive correlation coefficient between the two variables. The analysis of wavelet coherence corroborate with correlation analysis, as it showed in-phase covariance between wind speed and sediment concentration at the 12-month time scale and an out-of-phase covariance between sediment concentration and other forcings. Furthermore, the co-variance between  $R_{rs555}$  and river discharge

was not continuous. The higher importance of wind in both dispersion and intensity of plume is unusual if compared to findings of earlier studies on coastal plumes (Nezlin and DiGiacomo, 2005; Jabbar, et al., 2013; Saldías, et al., 2016; Mendes, et al., 2017). In those studies, the river discharge was found to be the main forcing and the wind was found to be the secondary forcing. As pointed out in the previous section, this pattern might be associated with the stationarity of Zambezi river flow due to regulation and sediment retention in the dam. The interannual variation is more pronounced in river discharge, which presents three distinct long-scale variations within the period of observation, comprising a period of relatively low flows, a period of high flows, and a period of intermediate flows. It is worth noting that there is a discrepancy between the Zambezi river discharge and rainfall over the Zambezi Delta, especially during the 2012–2014 period where the low river discharge rates coincide with high rainfall rates, probably due to flow regulation associated to water retention for electricity production and the fact that the rainfall regime upstream Zambezi Basin might be different to that of Zambezi Delta.

The outputs of one-way ANOVA are presented in Table 2, and they suggest that the  $R_{rs555}$  values in the north, center, and south regions of the Sofala Bank are statistically different ( $F$  calculated  $> F$  critical) with higher values observed in the south region ( $R_{rs555} = 0.0137 \text{ Sr}^{-1}$ ) and lower values observed in the central region near the Zambezi Delta ( $R_{rs555} = 0.0119 \text{ Sr}^{-1}$ ). The high  $R_{rs555}$  values in the south region might be associated with the relatively higher importance of Pungue and Buzi Rivers than the dammed Zambezi River in supplying sediments, and to higher re-suspension rates due to local tide ranges, dredging activities, and shallower bathymetry

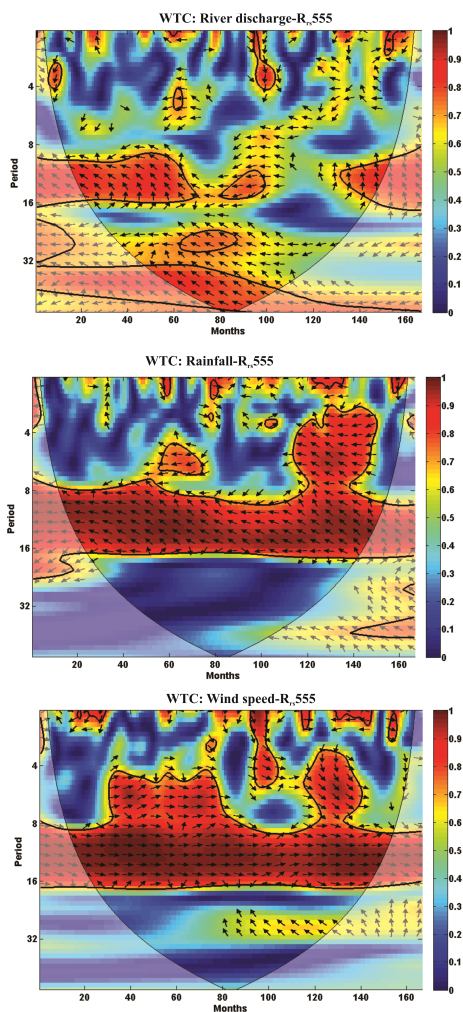


**FIGURE 7**  
Wavelet transform coherence between environmental variables and  $R_{rs555}$ : river discharge– $R_{rs555}$  (upper panel), Rainfall– $R_{rs555}$  (middle panel), and wind speed– $R_{rs555}$  (lower panel). The regions with significant edge influence are shaded. The arrows indicate the phase difference between the time series. When the two time series are in phase ( $0^\circ$ ), the arrows point to the right; when two time series are out of phase ( $180^\circ$ ), the arrows point to the left. The color bar indicates the variation of correlation coefficient.

observed in the south Sofala Bank. However, with the data and methods used in this research, no definitive conclusion can be drawn.

## Conclusions

In this study, we used remote sensing reflectance at 555 nm to evaluate the variability of coastal plume in the Sofala Bank and its relation to the Zambezi River discharge, rainfall in Zambezi Delta, and local wind speed. The use of monthly means of  $R_{rs555}$ , conditioned by poor availability of daily images due to cloud and other contamination, certainly did not allow the observation of maximum spatial extent of the coastal plume. Nevertheless, it was possible to have a general view of the temporal variability of both plume length and  $R_{rs555}$  signal intensity, which can hardly be accessed only using *in situ* observations. The coastal plume is relatively narrower, with lower  $R_{rs555}$  values during January–May, and it is wider, with higher  $R_{rs555}$  values during June–December, a time when smaller plumes are observed in front of the mouth of Buzi and Pungue rivers as well as in front of the mouth of the Licungo River. Comparison of  $R_{rs555}$  values in the north, center, and south region of the Sofala Bank revealed that the southern region under influence of Buzi and Pungue Rivers presents the highest values if compared to the center region located near the Zambezi Delta. Contrary to most other studies that used the green band to map coastal plume and relate its variability to river discharge, rainfall, and wind speed and had the river discharge as the main forcing of both coastal plume dispersion and intensity, in the present study, the wind was found to be the main forcing of plume variability. The dominance of wind in controlling the variability of  $R_{rs555}$  values and the relatively greater contribution of Pungue and Buzi River in comparison to the Zambezi River in supplying sediments, also pointed out in previous studies, such as Beilfuss and Davies (1999) and Ronco et al. (2010), could be an evidence of a decreased supply of sediments from the Zambezi River, which might have started after the damming of the Zambezi Catchment. The implications of decreased river supply include decrease in

**TABLE 1** Statistical outputs of the regression of MODIS  $R_{rs555}$  against river discharge, rainfall in Zambezi Delta, and wind speed.

MODIS $R_{rs555}$	R. discharge	Rainfall	Wind speed
$R$	–0.21	–0.67	0.77
$R^2$	0.04	0.32	0.6
RMSE	0.0007	0.0006	0.0004
$p$ -value	0.005	0	0

TABLE 2 Monthly mean values of  $R_{rs555}$  for each region of the Sofala Bank and resulting variance analysis for a critical value of 0.001.

Parameter	North	Center	South	F calculated	F critical	p-value
$R_{rs555}$ ( $Sr^{-1}$ )	0.0124	0.0119	0.0137	36.6183	3.0137	0.00

nutrient availability in the Sofala Bank, and the likelihood of enhanced coastal erosion in the delta region. However, another study based on *in situ* data is recommended to complement and further validate the findings of the present study.

## Data availability statement

The original contributions presented in the study are included in the article. Further inquiries can be directed to the corresponding author.

## Author contributions

HM: literature review, data processing and interpretation, and manuscript preparation; FN: data processing and interpretation. CS: supervising support during project conception and evaluation of manuscript. EO: supervising, data collection, and processing. All authors contributed to the article and approved the submitted version.

## References

- Alikas, K., Ansko, I., Vabson, V., Ansper, A., Kangro, K., Uudeberg, K., et al. (2020). Consistency of radiometric satellite data over lakes and coastal waters with local field measurements. *Remote Sensing* 12, 616. doi: 10.3390/rs12040616
- Balasubramanian, S., Pahlevan, N., Smith, Binding, B. C., Schalles, J., Loisel, H., et al. (2020). Robust Algorithm for estimating total suspended solids (TSS) in inland and nearshore coastal waters. *Remote Sens. Environ.* 246, 111768. doi: 10.1016/j.rse.2020.111768
- Beilfuss, R. D., and Davies, B. R. (1999). "Prescribed flooding and wetlands rehabilitation in the Zambezi delta, Mozambique," in *Perspective and wetland rehabilitation*. Ed. S. William (Dordrecht, Netherlands: Springer Dordrecht), 143–158.
- Beilfuss, R., and dos Santos, D. (2001). *Program for the sustainable management of cahora bassa dam and the lower zambezi valley* (Baraboo, USA: International Crane Foundation).
- Bontempi, P. S., and Yoder, J. A. (2004). Spatial variability in SeaWiFS imagery of the south Atlantic bight as evidenced by gradients (fronts) in chlorophyll a and water-leaving radiance. *Deep Sea Res. Part II: Topical Stud. Oceanography* 51, 1019–1032. doi: 10.1016/S0967-0645(04)00098-0
- Chevane, C. M., Penven, P., Nehama, F. P. J., and Reason, C. J. C. (2016). Modelling the tides and their impacts on the vertical stratification over the sofala bank, Mozambique. *Afr. J. Mar. Sci* 38, 465–479. doi: 10.2989/1814232X.2016.1236039
- Davies, B. R., Beilfuss, R. D., and Thoms, M. C. (2000). Cahora bassa retrospective 1974 1997: effects of flow regulation on the lower Zambezi river. *Limnol. Develop. World* 27, 1–9. doi: 10.1080/03680770.1998.11901620
- Durand, N., Fiandrino, A., Fraunié, P., Quillon, S., Forget, P., and Naudin, J. J. (2002). Suspended matter dispersion in ebro ROFI: an integrated approach. *Continental Shelf Res.* 22, 267–284. doi: 10.1016/S0278-4343(01)00057-7
- Fernandez-Nóvoa, D., Gomez-Gesteira, M., Mendes, R., deCastro, M., Vaz, N., and Dias, J. M. (2017). Influence of main forcing affecting the tagus turbid plume under high river discharges using MODIS imagery. *PLoS One*; 12, 1–27. doi: 10.1371/journal.pone.0187036
- Flemming, B. W., and Hermann-Rudolf, K. (2017). Large Dunes on the outer shelf off the Zambezi delta, Mozambique: evidence for the existence of a Mozambique current. *Geo Mar. Lett* 38, 95–106. doi: 10.1007/s00367-017-0515-5
- Gammelsrod, T. (1996). "Effect of Zambezi river management on the prawn fishery of the sofala," in *Water management and*. Eds. M. C. Acreaman and G. E. Hollis (Gland Switzerland: IUCN), 119–124.
- Gholizadeh, M. H., Melesse, A. M., and Reddi, L. A. (2016). Comprehensive review on water quality parameters estimation using remote sensing techniques. *Sensors* 16, 1298. doi: 10.3390/s16081298
- Grinsted, A., Moore, J. C., and Jevrejeva, S. (2004). Application of the cross wavelet transform and wavelet coherence to geophysical time series. *Nonlinear Processes Geophys.* 11, 561–566. doi: 10.5194/npg-11-561-2004
- Halo, I., Backeberg, B., Penven, P., Anson, I., Reason, C., and Ullgren, J. E. (2014). Eddy properties in the Mozambique channel: A comparison between observations and two numerical ocean circulation models. *Deep Sea Res. II* 100, 38–53. doi: 10.1016/j.dsr2.2013.10.015
- Hogwane, A. M. (2007). Perfil diagnóstico da zona costeira de moçambique. *Rev. Gestão Costeira Integrada* 7 (1), 69–82. doi: 10.5894/rgci11
- Hu, C., Feng, L., and Lee, Z. (2013). Uncertainties of SeaWiFS and MODIS remote sensing reflectance: Implications from clear water measurements. *Remote Sens. Environ.* 133, 168–182. doi: 10.1016/j.rse.2013.02.012
- Adler, R. F., Bolvin, D. T., Gu, G., Nelkin, E. J., Bowman, K. P., and Hong, Y. (2007). The TRMM multisatellite precipitation analysis (TMPA): Quasi global, multiyear, combined-sensor precipitation estimates at fine scales. *J. Hydrometeorol.* 8, 38–55. doi: 10.1175/JHM560.1

## Funding

The publication of this manuscript was made possible with financial support of the Mozambican Research Fund.

## Conflict of interest

The authors declare that the research was conducted in the absence of any commercial or financial relationships that could be construed as a potential conflict of interest.

## Publisher's note

All claims expressed in this article are solely those of the authors and do not necessarily represent those of their affiliated organizations, or those of the publisher, the editors and the reviewers. Any product that may be evaluated in this article, or claim that may be made by its manufacturer, is not guaranteed or endorsed by the publisher.

- IOCCG (2019). "Uncertainties in ocean colour remote sensing," in *IOCCG report series, no. 18*. Ed. F. Mélin (Dartmouth, Canada: International Ocean Colour Coordinating Group). doi: 10.25607/OBP696
- Jabbar, A., Lihan, T., Mustapha, M. A., Rahman, Z. A., and Rahim, S. A. (2013). Variability of river plume signature determined using satellite images. *J. Appl. Sci.* 13 (1), 70–78. doi: 10.3923/jas.2013.70.78
- Kalnay, E., Kanamitsu, M., Kistler, R., Collins, W., Deaven, D., et al. (1996). The NCEP/NCAR 40-year reanalysis project. *Bull. Amer. Meteor. Soc.* 77, 437–71.
- Klemas, V. (2012). Remote sensing of coastal plumes and ocean fronts: Overview and case study. *J. Coast. Res.* 28, 1–7. doi: 10.2112/JCOASTRES-11-00025.1
- Kolasinski, J., Kaehler, S., and Sébastien, J. (2012). Distribution and sources of particulate organic matter in a mesoscale eddy dipole in the Mozambique channel (south western Indian ocean): Insight from carbon and nitrogen stable isotopes. *J. Mar. Syst.* 122–131. doi: 10.1016/j.jmarsys.2012.02.015
- Lihan, T., Saitoh, S., Lida, T., Hirawake, T., and Lida, K. (2008). Satellite-measured temporal and spatial variability of the Tokachi River plume. *Estuar. Coast. Shelf Sci.* 78, 237–249.
- Liu, W.-C., Cheng, R. T., and Hsu, M.-H. (2008). Modelling the impact of wind stress and river discharge on danshuei river plume. *Appl. Math. Model.* 32, 1255–1280. doi: 10.1016/j.apm.2007.03.009
- Lutjeharms, J. R. E. (2006). "The coastal ocean of the south-Eastern Africa," in *The Sea*, vol. 14B. Eds. A. R. Robinson and K. H. Brink (Cambridge: Harvard University Press), 783–834.
- Lutjeharms, J. R. E., Blastoch, A., van der Werf, P. M., Ridderinkhof, H., and De Ruijter, W. P. M. (2012). On the discontinuous nature of the Mozambique channel. *South Afr. J. Sci.* 108, 5. doi: 10.4102/sajs
- Machaieie, H. A. (2012). "Water masses, circulation, stratification and fronts in sofala bank," in *MSc Dissertation, quelimane, Mozambique* (Quelimane, Mozambique: School of Coastal and Marine Sciences, Eduardo Mondlane University).
- Machaieie, H. A. (2018). "Assessment of spatial and temporal variability of satellite-estimated suspended sediment and chlorophyll over sofala bank, Mozambique, and their relation to environmental variables," in *Ph.D thesis*. Ed. R. J. Niteroi (Niteroi, Brazil: Fluminense Federal University, Department of Geology and Geophysics).
- Mendes, R., Saldias, G. S., deCastro, M., Gómez-Gesteira, M., Vaz, N., and Dias, J. M. (2017). Seasonal and interannual variability of the douro turbid river plume, northwestern Iberian peninsula. *Remote Sens. Environ.* 194, 401–411. doi: 10.1016/j.rse.2017.04.001
- Nehama, F. P. (2012). *Modelling the Zambezi river plume using the regional oceanic model system* (Ph.D Thesis, Cape Town, South Africa: Faculty of Sciences, Cape Town University).
- Nehama, F. P. J., Lemos, M. A., and Machaieie, H. A. (2015). Water mass characteristics in a shallow bank highly influenced by river discharges: the sofala bank in Mozambique. *J. Integrated Coast. Zone Manag.* 15, 523–532. doi: 10.5894/rgci560
- Hagen, E., da Silva, J. A., Schemainda, R., Michelchen, N., Kaiser, W., et al. (1987). Results of oceanological studies in the Mozambique channel in February – march 1980. *Beitr. Meereskd* 56, 51–63.
- Nezlin, N. P., and DiGiacomo, P. M. (2005). Satellite ocean color observations of stormwater runoff plumes along the San Pedro shelf (southern California) during 1997–2003. *Continental Shelf Res.* 25, 1692–1711. doi: 10.1016/j.csr.2005.05.001
- IOCCG (2020). "Synergy between ocean colour and Biogeochemical/Ecosystem models," in *IOCCG report series, no. 19*. Ed. S. Dutkiewicz (Dartmouth, Canada: International Ocean Colour Coordinating Group). doi: 10.25607/OBP-711
- Piola, A. R., Romero, S. I., and Zajaczkowski, U. (2008). Space–time variability of the plata plume inferred from ocean color. *Continental Shelf Res.* 28, 1556–1567. doi: 10.1016/j.csr.2007.02.013
- Pugh, D. (1987). *Tides, surges and mean Sea level: A handbook for engineers and scientists* (Chichester: John Wiley & Sons).
- Ronco, P., Fasolato, G., Nones, M., and Silvio, G. D. (2010). Morphological effects of damming on lower Zambezi river. *Geomorphology*; 115, 43–55. doi: 10.1016/j.geomorph.2009.09.029
- Saetre, R. (1985). Surface currents in the Mozambique channel. *Deep Sea Res.* 32, 1457–1467. doi: 10.1016/0198-0149(85)90097-4
- Saetre, R., and Jorge da Silva, A. (1982). Water masses and circulation on the Mozambique channel. *Rev. Investigação Pesqueira* 3, 1–83.
- Saldias, G. S., Sobarzo, M., Largier, J. L., Mendes, R., Pérez-Santos, I., and Vargas, C. A. (2016). Satellite-measured interannual variability of turbid river plumes off central-southern Chile: Spatial patterns and the influence of climate variability. *Prog. Oceanography* 146, 212–222. doi: 10.1016/j.pocean.2016.07.007
- Saldias, G. S., Sobarzo, M., Largier, J., Moffat, C., and Letelier, R. (2012). Seasonal variability of turbid river plumes off central Chile based on high-resolution MODIS imagery. *Remote Sens. Environ.* 123, 220–233. doi: 10.1016/j.rse.2012.03.010
- Schulz, H., Luckge, A., Emeis, K.-C., and Mackensen, A. (2011). Variability of Holocene to late pleistocene Zambezi riverine sedimentation at upper continental slope off Mozambique. *Mar. Geol.* 286, 21–34. doi: 10.1016/j.margeo.2011.05.003
- Siddorn, J. R., Bowers, D. G., and Hogue, A. M. (2001). Detecting the Zambezi river plume using observed optical properties. *Mar. pollut. Bull.* 42, 942–950. doi: 10.1016/S0025-326X(01)00053-4
- Silvada, A. J. (1984). Hydrology and fish distribution at sofala bank (Mozambique). *Rev. Investigação Pesqueira* 12, 5–36.
- Stramski, D., and Wozniak, S. B. (2005). On the role of colloidal particles in light scattering in the ocean. *Limnol. Oceanography* 50, 1581–1591. doi: 10.4319/lo.2005.50.5.1581
- Tan, C. K., Ishizaka, J., Matsumura, S., Yusoff, F. Md., and Mohamed, M. I. H. J. (2006). Seasonal variability of SeaWiFS chlorophyll a in the malacca straits in relation to Asian monsoon. *Continental Shelf Res.* 26, 168–178. doi: 10.1016/j.csr.2005.09.008
- Toole, D. A., and Siegel, D. A. (2001). Modes and mechanisms of ocean color variability in Santa Barbara channel. *J. Geophys. Res.* 106, 26985–27000. doi: 10.1029/2000JC000371
- Warrick, J. A., and Fong, D. A. (2004). Dispersal scaling from world's rivers. *Geophys. Res. Lett.* 31, L04301. doi: 10.1029/2003GL019114
- Warrick, J. A., DiGiacomo, P. M., Weisberg, S. B., Nezlin, N. P., Mengel, M. J., Jones, B. H., et al. (2007). River plume patterns and dynamics within the Southern California Bight. *Cont. Shelf Res.* 27, 2427–2448. doi: 10.1016/j.csr.2007.06.015
- Weiss, D. J. (2006). *Analysis of variance and functional measurement: A practical guide* (New York: Oxford University press).
- WWF (2004). *Towards a Western Indian ocean dugong conservation strategy: the status of dugongs in the Western Indian ocean region and priority conservation actions* (Dar es Salaam, Tanzania: WWF).